Author/s:
Sinclair, L;Lewis, V;Collins, SJ;Haigh, CL

Title:
Cytosolic caspases mediate mislocalised SOD2 depletion in an in vitro model of chronic prion infection

Date:
2013-07-01

Citation:
Sinclair, L., Lewis, V., Collins, S. J. & Haigh, C. L. (2013). Cytosolic caspases mediate mislocalised SOD2 depletion in an in vitro model of chronic prion infection. Dmm Disease Models and Mechanisms, 6 (4), pp.952-963. https://doi.org/10.1242/dmm.010678.

Persistent Link:
https://hdl.handle.net/11343/50194

RESEARCH ARTICLE

Disease Models & Mechanisms 6, 952-963 (2013) doi:10.1242/dmm.010678

Cytosolic caspases mediate mislocalised SOD2 depletion in an *in vitro* model of chronic prion infection

Layla Sinclair[1], Victoria Lewis[1], Steven J. Collins[1,*] and Cathryn L. Haigh[1,*]

SUMMARY

Oxidative stress as a contributor to neuronal death during prion infection is supported by the fact that various oxidative damage markers accumulate in the brain during the course of this disease. The normal cellular substrate of the causative agent, the prion protein, is also linked with protective functions against oxidative stress. Our previous work has found that, in chronic prion infection, an apoptotic subpopulation of cells exhibit oxidative stress and the accumulation of oxidised lipid and protein aggregates with caspase recruitment. Given the likely failure of antioxidant defence mechanisms within apoptotic prion-infected cells, we aimed to investigate the role of the crucial antioxidant pathway components, superoxide dismutases (SOD) 1 and 2, in an *in vitro* model of chronic prion infection. Increased total SOD activity, attributable to SOD1, was found in the overall population coincident with a decrease in SOD2 protein levels. When apoptotic cells were separated from the total population, the induction of SOD activity in the infected apoptotic cells was lost, with activity reduced back to levels seen in mock-infected control cells. In addition, mitochondrial superoxide production was increased and mitochondrial numbers decreased in the infected apoptotic subpopulation. Furthermore, a pan-caspase probe colocalised with SOD2 outside of mitochondria within cytosolic aggregates in infected cells and inhibition of caspase activity was able to restore cellular levels of SOD2 in the whole unseparated infected population to those of mock-infected control cells. Our results suggest that prion propagation exacerbates an apoptotic pathway whereby mitochondrial dysfunction follows mislocalisation of SOD2 to cytosolic caspases, permitting its degradation. Eventually, cellular capacity to maintain oxidative homeostasis is overwhelmed, thus resulting in cell death.

INTRODUCTION

The transmissible spongiform encephalopathies (TSEs; also known as prion diseases) encompass a group of fatal neurodegenerative diseases that differ from other dementias, such as Alzheimer's disease, because of their transmissible nature. The causative agent is composed wholly or largely of misfolded conformers of the prion protein (PrP) (Prusiner, 1982; Weissmann et al., 1994). These misfolded conformers (PrP^{Sc}) form a template for the cellular isoform of PrP (PrP^{C}) to misfold and in this way propagate themselves, resulting in the transmissibility of the TSEs.

Similar to other neurodegenerative diseases, prion disease in mice and humans is associated with markers of oxidative stress in the brain (Wong et al., 2001; Freixes et al., 2006), which increase concurrently with disease-associated PrP burden (Brazier et al., 2006). The oxidative stress has been attributed to an increased production of reactive oxygen species (ROS) due to metal ion dyshomeostasis and resulting redox activity (reviewed in Singh et al., 2010), changed redox signalling through NADPH oxidase (Schneider et al., 2003; Mouillet-Richard et al., 2007) and alterations in nitric oxide synthase (Park et al., 2011). PrP itself has been linked with an antioxidant function; possibly due to an inherent superoxide dismutase (SOD)-like activity (Brown et al., 1999) or by modulation of protective signal transduction pathways (Mouillet-Richard et al., 2007; Rachidi et al., 2003). Aside from a potential PrP SOD-like function, the cell has two further intracellular SODs: SOD1 (CuZnSOD) and SOD2 (MnSOD). SOD2 is localised within the mitochondria, whereas SOD1 has a more ubiquitous localisation (Kawamata and Manfredi, 2010). Reduced SOD activity is reported in prion protein knockout mice and cell cultures (Brown et al., 1997; Brown and Besinger, 1998; Klamt et al., 2001; Sakudo et al., 2005), and a loss of SOD function is one proposed mechanism of prion disease pathogenesis. Alterations in activity and redistribution to mitochondria is reported for SOD1 mutants associated with genetic amyotrophic lateral sclerosis (ALS) in humans and mice (Carrì and Cozzolino, 2011; Goldsteins et al., 2008) indicating that mislocalisation and altered activity of the SOD enzymes can have deleterious consequences for neurons.

Our previous work defined four stages of oxidative response in cultured cells exposed to infectious prions: acute, adaptive, chronic and terminal (Haigh et al., 2011). In these phases the oxidative state of the cell changes from oxidative stress to adaptational response to 'normal' oxidative capacity to loss of normal oxidative metabolism and increased ROS preceding death. The terminal subpopulation of cells accounts for ~6% of the chronically infected population and these cells show markers of apoptosis [phosphatidylserine (PS) externalisation] that correlate with detrimental oxidative stress, suggesting a possible failure of antioxidant compensatory responses. This apoptotic response is associated with the formation of aggregates of highly peroxidised lipid and activated caspases to which PrP is targeted. In this terminal phase of infection, the cells seem to be unable to maintain a defensive response to the increasing ROS burden, with a higher density of these aggregates appearing in apoptotic cells. We therefore sought to further investigate the role of the cellular

[1]Department of Pathology, Melbourne Brain Centre, The University of Melbourne, Victoria, 3010, Australia
*Authors for correspondence (stevenjc@unimelb.edu.au; chaigh@unimelb.edu.au)

Received 7 August 2012; Accepted 31 March 2013

TRANSLATIONAL IMPACT

Clinical issue

Prion diseases are aggressive, transmissible neurodegenerative disorders that often have long incubation periods. The causative agent of prion diseases, which can be transmitted through surgical procedures, blood transfusion or ingestion, is misfolded conformers of the normal cellular prion protein (PrP^{C}). These misfolded conformers (PrP^{Sc}) propagate themselves within their host by forming a template for the misfolding of PrP^{C}. The function of PrP^{C} and the mechanisms of toxicity during infection and prion propagation remain undefined, although both have been linked with cellular redox homeostasis. There is currently no effective treatment for prion diseases.

Results

Previous work by this group in a cellular model of prion infection showed distinct oxidative responses to infection that culminated in toxicity and cell death. Interestingly, in this model, despite an acute and damaging oxidative response to initial infection, prion propagation occurred in the bulk of the cellular population over a long period with only a subpopulation progressing to death, thereby emulating a long, asymptomatic incubation period. In the current study, the authors investigate the cellular response mechanisms that compensate for prion infection in their model and how these mechanisms fail in the cells that progress to death. Although the bulk population of prion-infected cells has an increased level of superoxidase dismutase (SOD; the SOD family helps to protect cells against oxidative damage) activity that is attributable to SOD1, this increased SOD activity is absent in the subpopulation of cells progressing to apoptosis. Interestingly, SOD2 (mitochondrial SOD) protein levels are reduced in the whole population as a result of mislocalisation to the cytosol and to aggregates containing caspases (enzymes involved in the execution of apoptosis) before progression to apoptosis and concomitant mitochondrial loss is observed. Notably, inhibition of caspases restores cellular levels of SOD2 in the infected cells.

Implications and future directions

These findings suggest that a failure of the cellular antioxidant response occurs during prion infection when SOD2 becomes mislocalised and available to cytosolic caspases. Although an increase in SOD1 activity can initially compensate for diminished SOD2 levels in mitochondria, subsequent failure of the SOD1 compensatory response results in mitochondrial damage, loss and ultimately cell death. These new insights into the cellular response mechanisms to prion propagation might help to explain why these diseases can have long asymptomatic incubation periods, and could also provide targets for the development of therapies for these fatal diseases.

antioxidant defence mechanisms in chronic and terminal prion infection *in vitro*. Primarily, we aimed to define the failure(s) in the adaptational response to chronic infection that result in the infected cells progressing to apoptosis. Our results suggest that chronic prion infection is associated with SOD2 mislocalisation, for which increased SOD1 activity compensates. The mislocalised SOD2 is directed to redox-active aggregates in the cytosol where it is degraded by caspases, resulting in a reduction of SOD2 protein levels. Eventually, mitochondria fail to cope with the lack of SOD2, which manifests as increased superoxide production, and ultimately mitochondrial numbers decline such that the cell can no longer maintain viability, resulting in the activation of apoptosis.

RESULTS

SOD1 activity increases in chronically infected cells and SOD2 protein levels decrease

moRK13 cells [rabbit kidney epithelial (RK13) cells expressing full-length murine PrP] readily propagate infectious prions and the line remains viable indefinitely, allowing the study of chronic cellular infection. Our previous work has shown that chronically infected cells do not show a difference in the overall production of intracellular ROS; however, increased ROS production is seen in a subpopulation of infected cells expressing apoptotic markers when separated from the predominant population (Haigh et al., 2011). To investigate the possibility that the greater population was maintaining normal ROS levels by increased antioxidant defences, we looked at intracellular total SOD activity in the infected and mock equal-passage moRK13 populations. All experimental data presented herein are generated using the moRK13 cell model unless otherwise stated. The SOD activity assay showed an increased activity in the infected cells (Fig. 1A); this activity was approximately double that seen in the mock cells. Confirming that the results were not a cell-specific effect, we also assayed differentiated murine neural stem cells (NSCs) for changes in total SOD activity after 5 days of exposure to infectious mouse brain homogenate (Fig. 1B). Increased SOD activity was found in these cultures, which displayed a PrP expression dependence. The NSCs were treated for only 5 days with infectious homogenate owing to the pronounced toxicity to these cells (Fig. 1C-E) (Haigh et al., 2011). In order to determine whether the increase in total SOD activity in the moRK13 cells was predominantly due to SOD1 or SOD2 or both, we used pharmacological intervention to inactivate each of the SODs individually. The doubled SOD activity in the infected cells is maintained when SOD2 is removed by precipitation out of the lysate but is lost when SOD1 is inactivated, indicating that SOD1 is contributing the increased SOD activity (Fig. 1F).

SOD1 and SOD2 protein levels within the mock and infected moRK13 cells were analysed by western blotting. Protein detection indicated that SOD2 levels were significantly decreased by around 50% in the infected cells (Fig. 1G), but SOD1 levels remained unchanged. When compared with the detected protein levels of each SOD, SOD2 activity was not changed relative to its expression levels. SOD1 activity was significantly increased but a concurrent increase in protein expression was not detected, indicating a possible allosteric modulation of SOD1 function (supplementary material Fig. S1).

Overall mitochondrial superoxide production is not changed in chronically infected cells

SOD2 is mitochondrially localised. With the protein levels of SOD2 decreased in the infected moRK13 cells as compared with the mock cells we sought to determine whether the mitochondria of these cells were experiencing greater oxidative stress. To measure the levels of superoxide within the mitochondria, MitoSOX fluorescent sensor probe was incubated in the live moRK13 cells and intensity levels determined. No significant difference between the mock and infected cells in mitochondrial superoxide production could be detected (Fig. 2A). This is consistent with our previously obtained results in these cells, which showed no difference in ROS production or evidence of oxidative stress between the mock and infected cells (Haigh et al., 2011). However, given the significant decrease in SOD2 protein levels, we queried whether other cellular changes might account for the apparent lack of change in mitochondrial superoxide; for example, rather than being due to maintenance of homeostasis, it might be a result of decreased numbers of

stressed mitochondria resulting in a 'normal' fluorescent signal (i.e. a lower quantity of mitochondria with a higher fluorescent signal). We therefore utilised two further mitochondrial probes: MitoTracker and Mito-RFP. The mitochondrial importation of both of these probes might be altered by the mitochondrial state of health (probe metabolism or active transport of probe), so both

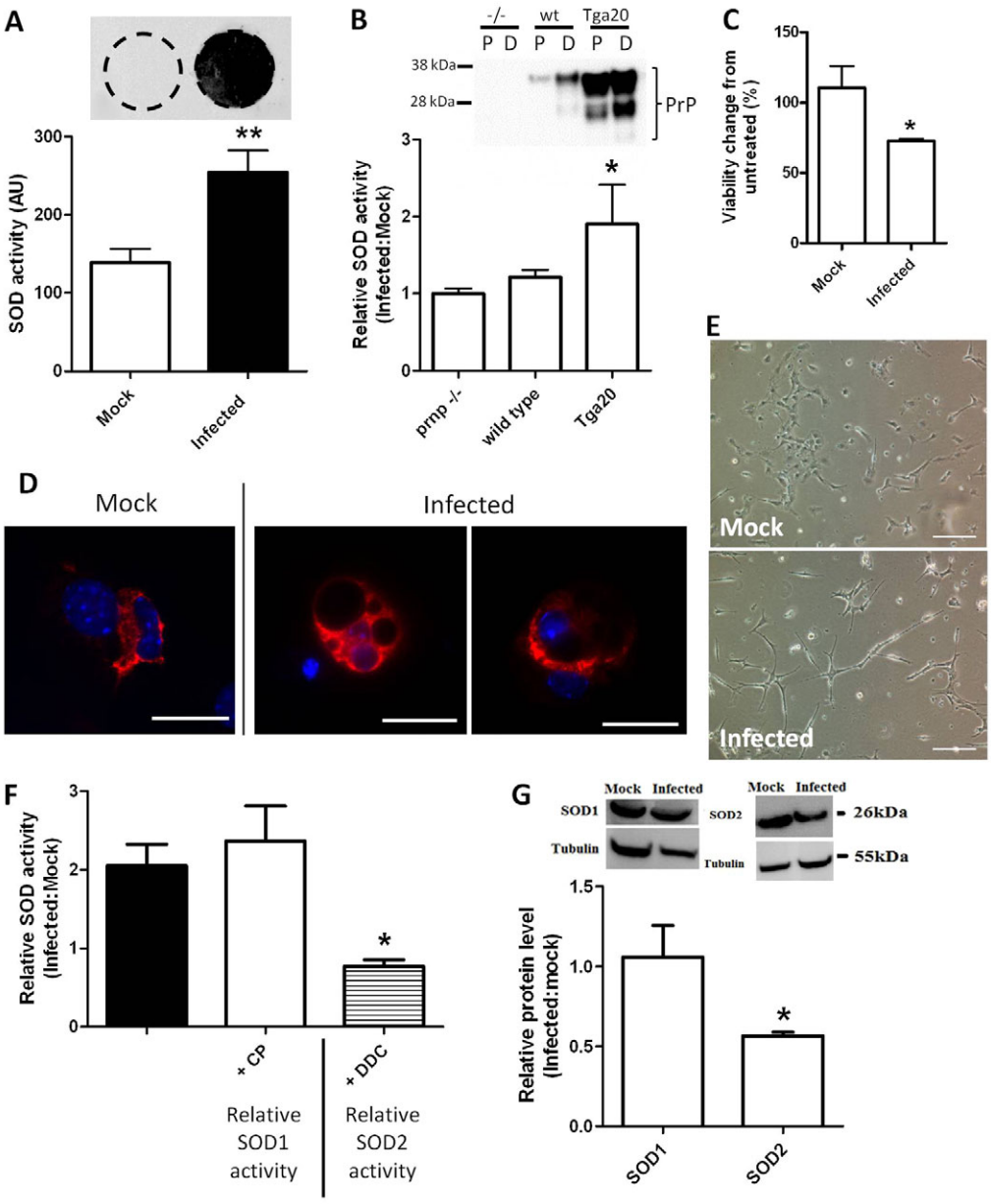

Fig. 1. Chronically infected cells demonstrate increased SOD1 activity and decreased SOD2 protein levels. (A) Chronically infected moRK13 cells show a heavy PrP^{Res} burden as detected by cell blot when compared with their mock-infected counterparts and increased total SOD activity (Student's *t*-test, t=3.46, $^{**}P$=0.0028, n=10). (B) NSCs derived from *prnp* knockout (–/–), wild-type (wt) and PrP overexpressor (Tga20) mice were differentiated into mature cultures and incubated for 5 days with mock or infectious brain homogenate. Tga20 cells exposed to infectious homogenate showed significantly increased SOD activity as compared with mock brain lysate controls (results are shown as ratios of infected to mock cell responses; Kruskal-Wallis K=6.038, $^{*}P$=0.0488, n=4). The magnitude of the SOD response correlated with PrP expression level, shown in the western blot above the SOD activity graph for comparison [duplicate lanes, proliferating cells left (P), differentiated cells right (D)]. (C) Wild-type NSCs were differentiated into mature cultures and exposed to mock or infectious inoculum for 24 hours. Cells exposed to infectious inocula demonstrate significantly reduced metabolic activity, as measured by MTS metabolism, relative to untreated or mock cells (t=2.421, $^{*}P$=0.036, n=3). (D) At 5 days post-addition of prion-infected inoculum, changes in cellular morphology were observed using fluorescence labelling of neuronal cells with antibodies targeting neurofilament-L (red); blue, DAPI. Scale bars: 25 µm. (E) Altered cellular morphology was also visible using brightfield microscopy. Scale bars: 50 µm. (F) SOD1 and SOD2 activities were differentiated using chloroform precipitation (CP) to isolate SOD1 from the lysate and addition of diethyldithiocarbamate (DDC) to inactivate SOD1. The results are shown as ratios of the infected to mock cell activities and show that SOD1 is primarily responsible for the increased activity observed (one-way ANOVA, F=5.796, $^{*}P$=0.012, n=3). (G) SOD protein levels were determined by western blotting and show SOD1 levels to be unchanged in the infected cells (Student's *t*-test, t=0.293, P=0.782, n=6) but SOD2 levels to be decreased (Student's *t*-test, t=18.67, $^{*}P$=0.0003, n=4).

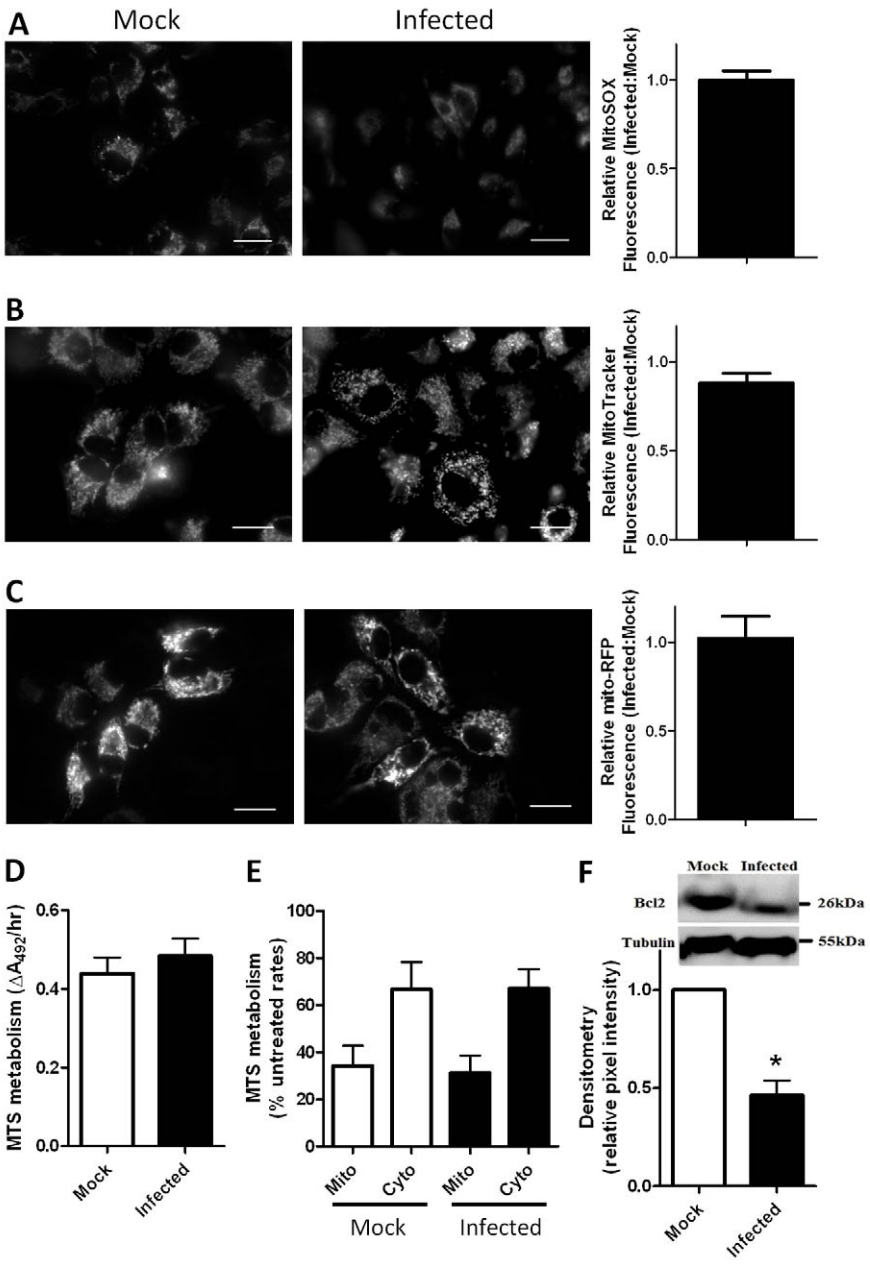

Fig. 2. Chronic prion infection does not influence mitochondrial superoxide production, numbers or metabolism but does reduce Bcl-2 protein levels. (A) MitoSOX, (B) MitoTracker and (C) Mito-RFP fluorescence (images) and intensity quantification, expressed as a ratio of infected to mock average cellular fluorescence (right of images), shows no change in mitochondrial superoxide production or mitochondrial numbers in the prion-infected cells compared with controls [Student's *t*-test; (A) t=0.027, P=0.98, n=4; (B) t=2.123, P=0.101, n=4; (C) t=0.179, P=0.869, n=4]. (D) MTS metabolism was unchanged in the prion-infected population compared with the mock control population (Student's *t*-test, t=0.749, P=0.466, n=4). (E) 1 nM rotenone and 10 μM DPI were used to inhibit mitochondrial and cytosolic metabolism, respectively. The mitochondrial (mito) and cytosolic (cyto) contributions to MTS reduction are not significantly different between the fractions (two-way ANOVA, F=0.0229, P=0.883, n=4). (F) Western blot analysis of Bcl-2 protein levels shows a reduction in prion-infected cells compared with controls (Mann-Whitney, U=0.00, *P=0.05, n=3). Black bars denote infected and white bars mock cells.

were considered together. No difference was found between the mock and infected moRK13 cells for either probe (Fig. 2B,C). As a further indication of mitochondrial stress, cellular metabolism of formazan was considered. Formazan metabolism occurs in both the mitochondria and the cytosol, so two inhibitors (rotenone, which indicates mitochondrial contribution by inhibiting NAD-linked substrate oxidation at the oxygen side of NADH dehydrogenase and DPI, an inhibitor of NADPH oxidase enzymes in the cytosol) were used to differentiate the mitochondrial contribution. Neither the cellular rate of formazan metabolism nor the mitochondrial contribution was altered in the infected moRK13 cells (Fig. 2D,E). Finally, we considered the mitochondrially localised anti-apoptotic protein Bcl-2, which has previously been linked with PrP binding and toxicity (Kurschner and Morgan, 1995; Rambold et al., 2006). This protein was decreased significantly in the infected moRK13 cells (Fig. 2F). Overall, it would seem that mitochondrial numbers, superoxide levels and function are maintained during chronic prion infection but with selective loss of SOD2 and Bcl-2.

SOD activity is increased in non-apoptotic infected cells only

In our previous study ROS levels were only found to be increased in the apoptotic subpopulation of infected moRK13 cells (Haigh et al., 2011). This population was only a small proportion of the entire culture population and changes in such a small number of cells might easily be missed; therefore, it was possible that SOD-activity was increased to compensate for the ROS insult in the dying cells only. Mock and infected moRK13 cells were separated based upon

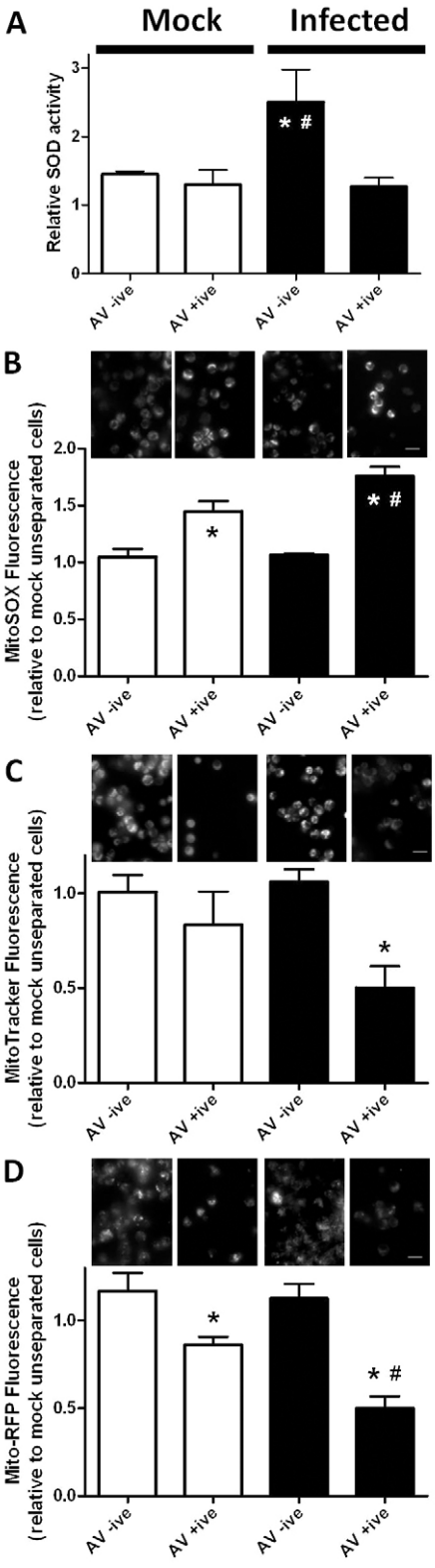

Fig. 3. An apoptotic population of prion-infected cells shows normal SOD activity but increased mitochondrial superoxide and decreased mitochondrial numbers. (A) Magnetic separation using annexin V (AV) to select the population of cells with externalised phosphatidylserine (a marker of apoptosis) showed the apoptotic fraction of prion-infected cells to have normal cellular SOD activities as compared with the mock-infected controls; the increased SOD activity was seen only in the non-apoptotic population (one-way ANOVA, F=4.402, P=0.036, n=4). (B) The apoptotic fraction of both the prion-infected and mock control cells showed increased mitochondrial superoxide over the non-apoptotic fraction and this was significantly greater in the prion-infected cells over the control cells (two-way ANOVA, F=23.56, P<0.001, n=4). (C,D) When mitochondrial numbers were considered with MitoTracker (C) and Mito-RFP (D) probes, signal was significantly reduced in the apoptotic prion-infected population (two-way ANOVA, F=4.493, P=0.025, n=4 and F=15.55, P=0.0002, n=4, respectively). * indicates significantly different to the non-apoptotic fraction, # indicates significantly different to the mock apoptotic fraction. Scale bars: 25 μm.

PS externalisation, a marker for apoptosis, and the SOD activity assays repeated. The opposite response to that hypothesised was observed, with increased SOD activity only observed in the non-apoptotic population of infected cells but not in the cells separated by their externalised PS and therefore committed to apoptotic cell death (Fig. 3A).

In the apoptotic subpopulation of infected cells, mitochondrial superoxide levels are increased and total mitochondria are decreased

Because the increased total SOD activity was not maintained in the apoptotic infected cells, it was plausible that, in the absence of appropriate antioxidant control, the mitochondrial superoxide production could be increased. Therefore, we tested the superoxide production in these cells using the MitoSOX probe. Although mitochondrial superoxide was increased in both populations of apoptotic moRK13 cells (mock and infected), the infected apoptotic cells showed significantly higher levels than the non-infected apoptotic cells (Fig. 3B). Examining these cells with the MitoTracker and Mito-RFP probes indicated that the apoptotic infected cells had lower numbers of mitochondria, as determined by lower fluorescence levels (Fig. 3C,D). Relatively, in the pro-apoptotic infected cells, fewer mitochondria were generating considerably more superoxide.

Mitochondrial SOD2 depletion is caused by SOD2 mislocalisation to the cytosol

Various pathways by which mitochondria can be lost are reported within the literature. Mitochondria can be extruded from cells by being engulfed in vesicles that are similar to autophagic vacuoles, with release into the surrounding milieu (Lyamzaev et al., 2008; Nakajima et al., 2008). To look for evidence of mitochondrial extrusion as the cause of their loss in the pro-apoptotic infected cells, conditioned media from the whole, unseparated moRK13 cell populations was western blotted for SOD2 and Bcl-2 as evidence that mitochondria were located outside of the cell. Although significant signal was seen for SOD2 in both the mock and infected conditioned media, and this was greater for the infected cells, there was no detectable Bcl-2, suggesting that mitochondria were not being extruded but SOD2 was being expelled from the cell by some other means (Fig. 4A).

Another mechanism by which mitochondria are lost in disease is through mitoptosis, considered the mitochondrial equivalent of apoptosis (Mijaljica et al., 2010; Tinari et al., 2007). In mitoptosis,

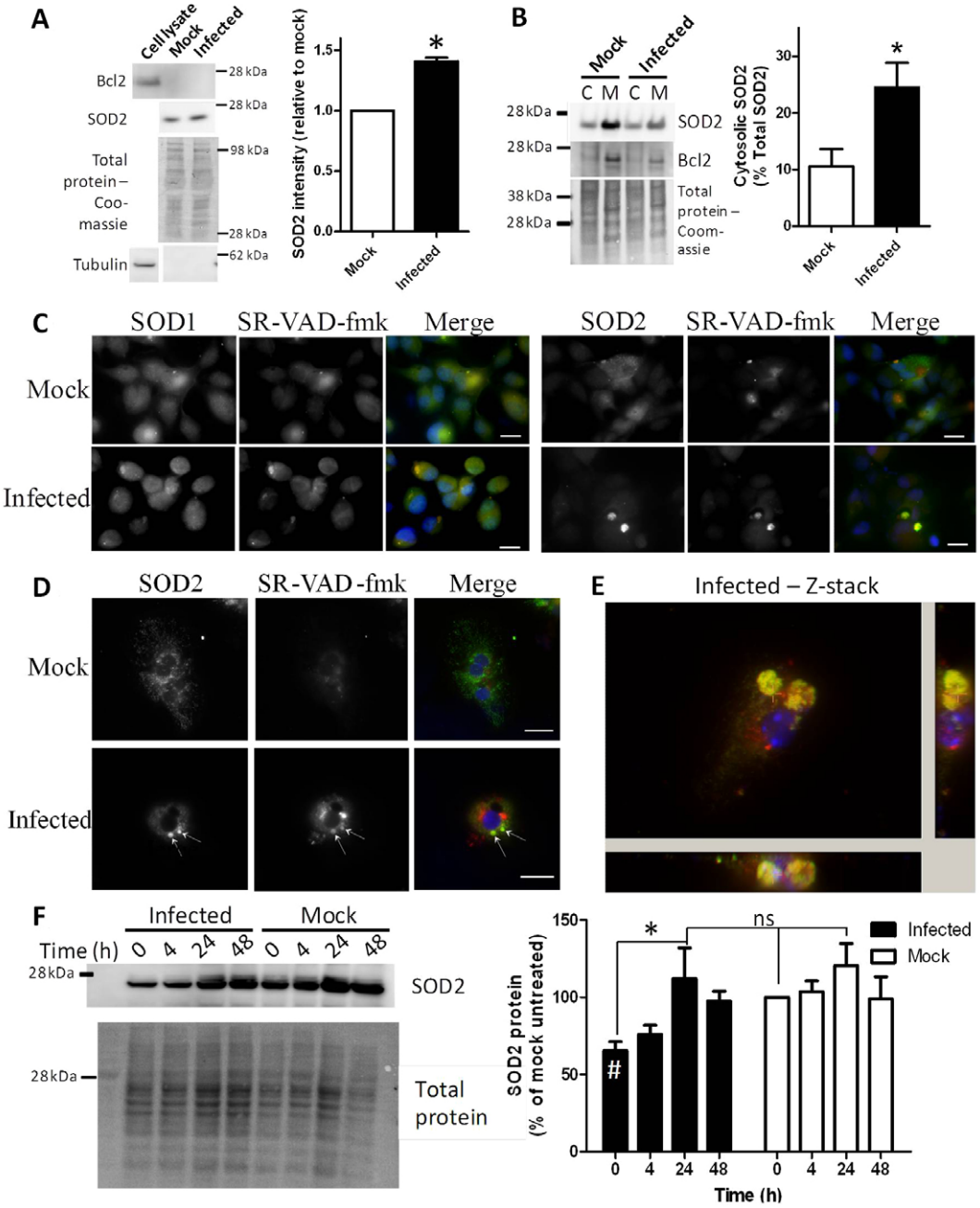

Fig. 4. SOD2 is mislocalised to the cytosol and degraded by caspases. (A) Western blotting of conditioned media shows that SOD2 is expelled from the cell in the absence of mitochondrial extrusion; this is significantly increased for the infected cells (Student's *t*-test, t=13.62, *P=0.0053, n=4). A lack of β-tubulin detection shows that conditioned media SOD2 detection is not due to cell contamination. (B) Separation of mitochondrial and cytosolic fractions demonstrates that SOD2 is found in the cytosol in relatively greater proportions in infected cells than uninfected as a result of depletion from the mitochondrial fraction (Student's *t*-test, t=2.702, *P=0.0427, n=4). Bcl-2 blotting shows that the cytosolic fraction is not highly contaminated with mitochondria. (C) Co-staining mock and infected cells with SR-VAD-FMK (pan caspase inhibitor; red in merge) and SOD1 or SOD2 (green in merge) shows SOD2 to be highly localised to caspase-reactive aggregates within the infected cells with very low detection elsewhere in the cell. Blue, DAPI. Scale bars: 25 µm. (D) Wild-type NSCs were differentiated then incubated with mock or infectious lysate for 5 days. After this time cells were incubated with SR-VAD-FMK then immunostained for SOD2. Cells exposed to infectious innocula display clumps of SOD2 colocalising with the caspase marker. Example mock and infected cell photomicrographs are shown; blue, DAPI; green, SOD2; red, SR-VAD-FMK; arrows indicate caspase-SOD2 clumps. Scale bars: 25 µm. (E) *z*-stack of a wild-type neural stem cell, exposed to infectious innoculum, containing large caspase-reactive aggregates. Colouring as for D; cross-hairs indicates sectioning. (F) Mock and infected cells were incubated with the pan-caspase inhibitor for 4, 24 or 48 hours and SOD2 protein levels determined by western blotting; left plate shows example blots and right plot shows densitometrical analysis normalised to mock time 0 expression levels. Incubation of mock and infected cells with the pan-caspase inhibitor for up to 48 hours significantly increases intracellular SOD2 at 24 hours (two-way ANOVA, F=7.78, *P=0.0038, n=4), restoring detection to that of the mock cells. $^{\#}$ indicates that SOD2 is significantly decreased in the untreated infected cell population (t=6.204, P=0.0084, n=4). Mock and infected cell responses to caspase inhibition are not significantly different to each other (ns, not significant; two-way ANOVA, F=2.194, P=0.164, n=4).

mitochondria can fragment, losing their outer membrane and releasing their contents into the cytosol, thus losing their functionality, or suffer fragmentation of the inner membrane leaving only a dysfunctional outer husk (Mijaljica et al., 2010; Tinari et al., 2007). Mitochondrial preparations of the whole, unseparated moRK13 cell populations were examined to look for evidence of SOD2 in the cytosol of infected cells as a result of leaky mitochondria. Western blotting showed that SOD2 was increased relative to total cellular SOD2 detection in the cytosol of the infected cells compared with their mock counterparts (Fig. 4B). Bcl-2 blotting confirmed minimal cross-contamination of the cytosolic fraction with the mitochondrial fraction (Fig. 4B), suggesting a selective relocalisation of SOD2.

SOD2 is degraded by caspases in the cytosol

Western blotting indicated a mislocalisation of SOD2 into the cytosol of infected cells, so immunofluorescence was used to image the location of both SOD1 and SOD2 in the cytosol of mock and infected moRK13 cells. Acknowledging that a change of location can be part of an apoptotic pathway, co-staining with a rhodamine-labelled pan-caspase inhibitor (SR-VAD-FMK) was also performed. Both SOD1 and SOD2 localise with the previously described (Haigh et al., 2011) caspase-positive aggregates within the infected cells but SOD2 shows a more pronounced colocalisation, with decreased levels of SOD2 elsewhere throughout the cell (Fig. 4C). SOD2 colocalisation with caspase-positive aggregates was also observed in cultures of differentiated wild-type NSCs exposed to infectious inoculum for 5 days (Fig. 4D,E). Immunofluorescent staining shows that cleaved (active forms of) caspases 3 and 9 localise with these aggregates but that pro-caspase 3 and caspase 6 show very little localisation (supplementary material Fig. S2). To test the hypothesis that SOD2 was being degraded by mislocalisation to the cytosolic caspase aggregates, the caspase inhibitor was used to block caspase activity for up to 48 hours. This treatment has previously been shown to increase the viability of these cells (Haigh et al., 2011). At 24 hours of caspase inhibitor treatment, the level of SOD2 protein within the cell was significantly increased (Fig. 4F), with detected levels in the infected cells restored to match those measured in the mock cells. Bcl-2 is also cleaved by caspase 3 to a Bax-like pro-apoptotic form (Cheng et al., 1997). Therefore, we also treated the mock and infected cells with the caspase inhibitor and also a radical scavenger, in case ROS production was also influencing Bcl-2 loss, at the 24-hour time point to see whether Bcl-2 also increased following treatment. No significant differences in Bcl-2 levels were observed in the treated infected cells compared with the untreated (supplementary material Fig. S3).

DISCUSSION

Previously, we have shown unchanged ROS levels in overall populations of infected cells compared with their mock counterparts during chronic prion infection; however, the cells in the acute or apoptotic terminal phase had higher ROS levels than the mock control cells (Haigh et al., 2011). Prompted by the observation that overall ROS levels were 'normal' during chronic infection but the apoptotic subpopulation showed oxidative stress, we investigated the cellular antioxidant defence pathways responsible for compensation to the chronic infection and the adaptational failure(s) associated with progression to apoptosis. Regulation of, or influence on, cellular SOD activity by PrP has been an important ongoing theme in prion infection and therefore SOD1 and SOD2 were the candidate molecules chosen for examination. SOD1 activity was increased and SOD2 protein levels decreased in chronically infected cells. SOD2 downregulation has previously been associated with prion infection *in vivo* (Choi et al., 1998; Lee et al., 1999; Park et al., 2011). Although these studies did not report an increase in SOD1 activity, regulation of SOD1 activity by PrP has also been reported (Brown et al., 1997; Sakudo et al., 2005) and SOD1 knockout has been shown to significantly reduce disease incubation time in murine models of prion disease (Akhtar et al., 2013). In the current system, the increased SOD1 activity might explain how the majority of moRK13 cells are able to remain viable in culture, despite reduced SOD2 levels, while propagating infection over long periods of time. The upregulated SOD response to infectious inoculum was also seen in the NSC cultures. The NSCs show an acute toxic response of increased ROS and decreased viability within 24 hours of exposure to infectious PrP (Fig. 1) (Haigh et al., 2011) and therefore were assayed after 5 days to allow a recovery period after the acute insult. Although it is not possible to discern whether it is *de novo* PrP^{Sc} propagation or PrP^{Sc} exposure that causes toxicity, those cells that survive to 5 days post-exposure have increased their antioxidant defences to compensate.

Given that SOD1 activity was increased in chronically infected cells, the subpopulation of apoptotic cells were separated from non-apoptotic cells to assess the activity in this apoptotic population, which has previously been shown to have increased ROS production (Haigh et al., 2011). The apoptotic population is relatively small compared with the non-apoptotic population, but still constitutes ~6% of infected cells, double the 3% of mock cells (Haigh et al., 2011), and so the responses of these cells can easily be overlooked because detection of these changes are overwhelmed by the remaining population. The total SOD activity in the infected apoptotic cells was not different from the levels seen in the mock cells (either separated or not); therefore, the overall increase in SOD1 activity must be due to the non-apoptotic population. This seems to indicate a relative decline in SOD activity in the infected apoptotic cells, thereby allowing detrimental ROS production within these cells, which contributes to their demise.

Mitochondrial respiration is one of the major cellular processes that produce ROS. Because levels of the mitochondrially localised SOD2 were decreased in chronically infected cells, mitochondrial representation within the cell was considered, but no difference was seen between the overall mock and infected populations. This lack of change is consistent with the investigations of Sisková et al., who found no prion-disease-associated changes in mitochondrial density or expression of mitochondrial proteins (Sisková et al., 2010). The same study did find changes to the mitochondrial inner membrane morphology and reduced cytochrome *c* oxidase activity, and similar observations were also made by others (Choi et al., 1998; Lee et al., 1999).

The pronounced loss of mitochondria in the pro-apoptotic prion-infected cells might indicate a primary contribution to cell death as part of the apoptotic response. Mitoptosis, the pathways of mitochondrial death, manifests in various ways (Lyamzaev et al., 2008; Nakajima et al., 2008). Although we saw evidence of SOD2 in conditioned media, there was no evidence for mitochondrial

extrusion, indicating that the cytosolic SOD2 was apparently independently being expelled from the cell. In the absence of other intracellular molecules, such as tubulin, this was probably a specific event as opposed to non-specific cell lysis or fragmentation. Colocalisation with active caspases in the previously reported oxidised aggregates (Haigh et al., 2011) indicated that SOD2 might be degraded when located outside the mitochondria. No evidence of mitochondria has ever been observed in these aggregates, additionally suggesting that the SOD2 is selectively mislocalised. Mislocalisation might be a result of mis-targeting of SOD2 to the cytosol following synthesis or could be due to loss from failing mitochondria. Furthermore, in the current study and as previously reported (Haigh et al., 2011), in cells in which the caspase reactive aggregates are observed there is no apparent depletion of mitochondria, indicating that the SOD2 relocalisation to the aggregates occurs while the mitochondria are still present and intact. Park et al. found reduced mitochondria in an *in vivo* model of prion disease, which occurred concurrently with a decrease in SOD2 (Park et al., 2011). Electron microscopy comparing infected and uninfected mouse brain tissue found evidence of loss of internal structures of the mitochondria. The authors correlated this with increased endothelial nitric oxide synthase (eNOS) and thus with increased intra-mitochondrial oxidative stress. This is consistent with our findings, but does not explain the relatively selective loss of the SOD2 protein from the mitochondria at a stage before mitochondrial function is apparently significantly compromised and the presence of this organelle depleted.

A decline in SOD2 protein level and function does not seem to be a prion-disease-specific pathway. Similar decreases are reported in other conditions of chronic oxidative stress such as heart failure, in which mRNA levels are increased but protein levels decreased (Holley et al., 2011; Sam et al., 2005), and osteoarthritis, in which SOD2 protein decreases precede erosion of cartilage (Scott et al., 2010). A paradigm attempting to recapitulate a generic model of chronic low-level oxidative stress using hydrogen peroxide exposure did not replicate a reduction in protein levels of SOD2 in the moRK13 cells (supplementary material Fig. S4), but rather an increase in SOD2 protein was instead observed. This might imply that the reduction in SOD2 protein levels in the chronic phase of prion infection requires much longer periods of time to manifest, or is caused by a specific ROS or reactive nitrogen species or localisation of these species, or that other dysfunctional pathways are also contributing to SOD2 protein level reduction. Further investigation is required to resolve these intricacies.

Caspase degradation of SOD2 has been reported as part of the extrinsic apoptotic pathways, with two caspase 3 cleavage sites identified within human SOD2 and recombinant caspase 3 shown to cleave recombinant SOD2 (Pardo et al., 2006). Activation of CD95 (also known as Fas) apoptotic pathways has been shown to redistribute PrP^{C} to mitochondria in lymphoid lineage cells (Mattei et al., 2011). Li et al. found that cytosolic PrP disrupts the proper formation of the cytoskeleton (Li et al., 2011). Together, the altered cytoskeleton and the direct PrP (or the disease-associated PrP^{Sc} isoforms) action on mitochondria might serve to mis-target SOD2 to the cytosol, permitting its incorporation into the caspase reactive aggregates and its loss into the surrounding cellular environment. Caspase 3 has also been shown to cleave Bcl-2 (Cheng et al., 1997) and could represent a common pathway, linking the decreases of SOD2 and Bcl-2. Interestingly, the resulting peptide formed by caspase 3 cleavage of Bcl-2 has Bax-like death effector function (Cheng et al., 1997) and might provide an explanation as to why prion-infected mice that overexpress Bcl-2 succumb to disease earlier than wild-type mice (Steele et al., 2007), apparently contrary to the expected anti-apoptotic function of Bcl-2. Although a pan-caspase inhibitor failed to restore Bcl-2 levels in our cell system (supplementary material Fig. S3), we cannot rule out that prion-infected cells downregulate protein expression of Bcl-2 to protect against deleterious consequences of caspase cleavage producing the pro-apoptotic form.

Evidence of caspase activation has been detected in brain tissue obtained post-mortem from human Creutzfeldt-Jakob disease (CJD) patients (Jesionek-Kupnicka et al., 1997; Puig and Ferrer, 2001) and can be observed in the brains of live mice in the pre-terminal phases of prion disease (Lawson et al., 2010), with caspase-reactive aggregates observed inside neurons using the same active caspase label as in the current study (Drew et al., 2011). Furthermore, in GT1 and N2a cell models of prion infection, aggresomes associated with increased caspases 3 and 8 activity are formed when the proteosome is inhibited (Kristiansen et al., 2005). The targeting of SOD2 to similar aggregates, with a loss of up to 50% of normal activity in the chronically infected cells, before any detectable decline in mitochondrial numbers is indicative of this event forming part of the toxic pathways that ultimately contributes to mitochondrial loss (as a result of superoxide accumulation) and cellular demise.

SOD2 knockout mice develop a neonatal lethal cardiomyopathy and metabolic acidosis within the first week of life; aside from the heart, post-mitotic tissues with high metabolic requirements including the brain are the most severely affected tissues (Lebovitz et al., 1996). Interestingly, if the mice are kept alive beyond the expected 1 week using antioxidant therapy, they develop an oxidative-stress-mediated spongiform encephalopathy (Melov et al., 1998). Complexes I-IV of the electron transport chain were found to have diminished activity and protein levels, which was pronounced for complex II, directly correlating with the dose of antioxidant used to prolong the life of the mouse (Hinerfeld et al., 2004). PrP knockout mice show increased superoxide production from complex I (Paterson et al., 2008). During prion disease, increased superoxide due to the conversion of PrP^{C} to PrP^{Sc}, coupled with a loss of SOD2 and therefore its antioxidant activity, might begin a cycle of heightened oxidative damage within mitochondria, eventuating in their loss. SOD2 mimetics have been proposed as potential therapeutics for prion disease (Fukuuchi et al., 2006). One such mimetic demonstrated an ability to extend the lifespan of prion-infected mice with reduced vacuolation within the hippocampus in early and terminal disease (Brazier et al., 2008), and therefore might indicate that a restoration of SOD2 function is crucial for cellular survival in prion disease. A schematic of potential cell death pathways enhanced by prion infection is shown in Fig. 5.

A further factor in this scenario is the heightened SOD1 activity in the non-apoptotic infected cells. As stated, this could represent a compensatory response that allows prolonged survival of cells in the same manner as using antioxidant therapy in SOD2 knockout mice. However, increased SOD1 activity might itself contribute to a loss of cellular ROS homeostasis with a potential toxic gain of

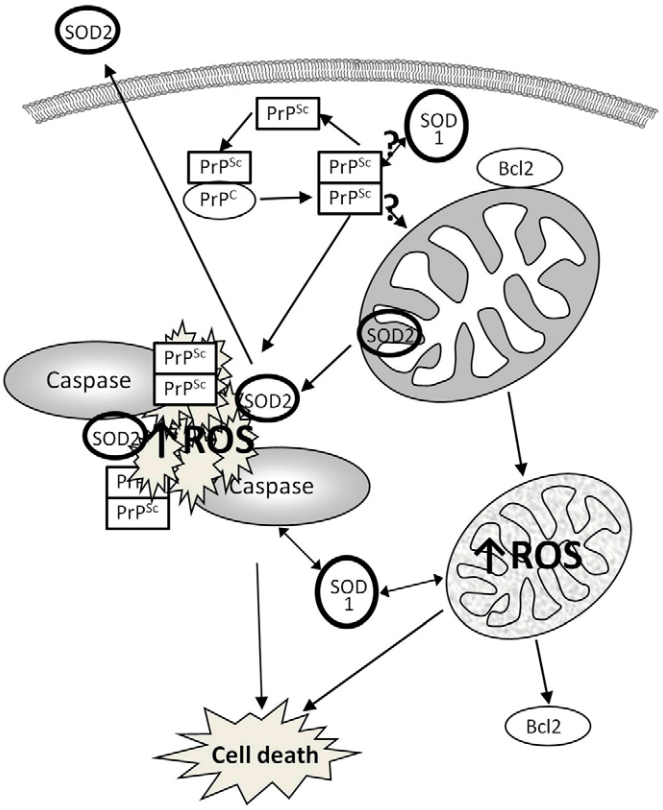

Fig. 5. Putative cell death pathway hijacked by prion infection. Schematic illustration of the potential death pathway enhanced by prion propagation.

function inadvertently contributing to cellular decline. In a murine model of ALS, in which mice express a mutant form of SOD1 displaying a toxic gain of function, the absence of PrP leads to decreased levels of Bcl-2 and vacuolation of motor neurons (Steinacker et al., 2010). These observations might indicate that an overactivity of SOD1 caused by or coinciding with a disturbance of a PrP regulatory function could be responsible for characteristic prion pathology and cellular demise. We did not observe any increased localisation of SOD1 in mitochondria of infected cells (data not shown), but cannot exclude that a gain of function is adversely affecting this organelle.

The mechanisms by which SOD2 is relocated from mitochondria and those responsible for the decline in mitochondrial numbers during terminal prion infection still remain to be revealed. The relocalisation might be a deliberate redirection by cellular targeting mechanisms to compensate for increased cytosolic oxidative flux or might be a side effect of the disease process. Overall, SOD2 mislocalisation seems to be an integral part of SOD2, mitochondria and ultimately cell loss in terminal prion infection.

In summary, elaborating on previous work, we believe that the present results support the contention that chronic prion infection is associated with relatively early loss of SOD2 from mitochondria, while organelle numbers and functionality are generally maintained. SOD2 is mislocalised to the cytosol where it is catabolised at least in part by caspases and also apparently undergoes increased selective extrusion from the cell through unclear mechanisms; overall cellular ROS homeostasis is maintained by compensatory increased SOD1 activity. Eventually, in a subset of chronically prion-infected cells, a deleterious cycle leads to initiation of apoptosis that is associated with prominent loss of mitochondria and heightened superoxide generation in the remaining dysfunctional mitochondria, culminating in the death of these cells.

MATERIALS AND METHODS

Cell culture

Rabbit kidney epithelial (RK13) cells expressing full-length murine PrP (moRK13) were generated as described previously (Haigh et al., 2009). Cells were routinely cultured in Dulbecco's modified Eagle's medium (DMEM; Invitrogen, Melbourne, VIC, Australia) supplemented with 10% (v/v) foetal bovine serum (Lonza, Australia), 50 U/ml penicillin/50 µg/ml streptomycin solution (Sigma, Melbourne, VIC, Australia) and 2.5 µg/ml puromycin (Sigma). Cell cultures were maintained at 37°C with 5% CO_2 in a humidified incubator.

Stem cell culture

Neural stem cells (NSCs) were harvested from c57BL/6×SV129 mice of *prnp*$^{-/-}$ (prion gene knockout) (Büeler et al., 1993), wild type or Tga20 (transgenic prion overexpression of approximately eightfold at the protein level) (Fischer et al., 1996) genetic background, as described in Haigh et al. (Haigh et al., 2011). NSCs were maintained in Neurocult complete proliferation medium (Stem Cell Technologies, Melbourne, VIC, Australia) at 37°C with 5% CO_2 in a humidified incubator. Differentiation was induced by transferral of cells into Neurocult complete differentiation medium (Stem Cell Technologies) and plating on a poly-D-lysine matrix (Sigma-Aldrich).

Cell infections

Cells were infected with the M1000 mouse adapted, human GSS-derived strain of prions or 'mock-infected' with normal brain homogenate (Lawson et al., 2008; Lewis et al., 2009) and permitted to propagate infection until the infected population was uniformly laden with protease-resistant PrP (PrP^{Res}; approximately >passage 50), a marker of propagating prions, as determined by cell blot assay (Fig. 1A). These cells are referred to as 'mock' or 'infected' throughout. *De novo* infections with M1000 were prepared by centrifugal collection of M1000-infected and mock-infected cells (300 ***g*** for 5 minutes), followed by washing in Dulbecco's phosphate buffered saline (dPBS; Invitrogen) and centrifugation as before. Lysate pellets were weighed and a 10% wet pellet weight/volume homogenate made in dPBS. Naïve cells were overlaid with 0.01 or 0.1% (w/v) of the mock or M1000-infected homogenised lysate. Cells were returned to the incubator until they were ready to be passaged. Long-term infection (empirically determined by cell blotting, see below) is defined as greater than passage 50. New infections were routinely established to ensure cell drift did not bias results.

SOD activity assay

Samples were prepared by washing cells in dPBS, followed by lysis with ice-cold 0.1 M Tris/HCl, pH 7.4 containing 0.5% (v/v) Triton X-100, and 0.1 mg/ml of Complete Mini, EDTA free, Protease Inhibitor Tablets (Roche, Melbourne, VIC, Australia). Cell lysates

were briefly centrifuged to separate membrane and nuclear debris and the supernatant collected for use in the assay. Determination of SOD activity was performed as described by the Superoxide Dismutase Activity Colorimetric Assay Kit protocol (Abcam, Sapphire Biosciences, Sydney, NSW, Australia).

Differentiating SOD1 and SOD2 activity

SOD1 and SOD2 activity discrimination utilised chloroform precipitation of SOD1 (SOD2 does not survive this treatment) and inclusion of diethyldithiocarbamate (DDC; Sigma) in the sample buffer to deactivate SOD1. For chloroform precipitation, 96 µl of ice-cold 37.5/62.5 (v/v) chloroform/ethanol solution was added to 60 µl of cell lysate. Samples were centrifuged for 10 minutes at 1000 ***g*** at 4°C and the aqueous phase was removed and stored at 4°C until use. SOD1 inhibition was achieved by the addition of DDC to 1 mM final concentration. Remaining SOD activity in these samples was measured as above.

Preparation of conditioned media

Cells were transferred into serum-free OptiMEM overnight (16 hours) and incubated under normal conditions. Media was collected and centrifuged at 150 ***g*** for 3 minutes to remove any cell carcasses. The media was then transferred to a fresh tube and mixed with four equivalent volumes of ice-cold methanol then stored at –20°C overnight. The precipitated protein was collected by centrifugation at 3273 ***g*** for 1 hour. Protein pellets were solubilised in 1× NuPAGE gel loading buffer (Invitrogen) with 5% (v/v) β-mercaptoethanol.

Mitochondrial preparations

Mitochondria and cysolic preparations were separated by washing cells briefly in dPBS, then collecting the cell suspension in phosphate buffered saline (PBS) by centrifugation at 335 ***g*** for 5 minutes. The cell pellet was resuspended in hypotonic buffer (10 mM NaCl, 1.5 mM $CaCl_2$, 10 mM Tris, pH 7.5) and lysed on ice by needle aspiration 20 times through an 18-gauge needle. One quarter sample volume of 5× sucrose solution (1.65 M sucrose, 30 mM EDTA, 43 mM Tris, pH 7.5) was added to the homogenate and the sample mixed. Nuclei and unbroken cells were separated by centrifugation at 600 ***g*** for 10 minutes. The supernatant was transferred to a fresh tube and centrifuged for 10 minutes at 10,000 ***g***. The supernatant (cytosolic fraction) was collected and the pellet (mitochondria) resuspended in 1× sucrose solution.

Western blotting

Cells were lysed in RIPA buffer [50 mM Tris-HCl pH 7.4, 150 mM NaCl, 0.1% (w/v) SDS, 0.5% (w/v) sodium deoxycholate, 1% (v/v) NP-40] at 37°C for 20 minutes. Samples were electrophoresed using the NuPAGE system (Invitrogen), transferred onto PVDF (Millipore) membranes and blocked as described previously (Haigh et al., 2009) with the exception of PrP blots, which used 2% (w/v) ECL Advance buffer with ECL Advance developer (GE Healthcare, Sydney, NSW, Australia). Protein of interest detection was made using the following dilutions of primary antibody: 1 in 2000 SOD1 (Abcam); 1 in 5000 SOD2 (Abcam); 1 in 1000 Bcl-2 (GE Healthcare); 1 in 5000 EP1802Y against PrP (Abcam) and 1 in 10,000 β-tubulin (Sigma-Aldrich) in PBS with 0.1% (v/v) Tween-20 (PBS-t). Secondary antibodies (Dako, Melbourne, VIC, Australia) were used at 1 in 5000 anti-rabbit (SOD1, SOD2), 1 in 10,000 anti-rabbit (PrP), 1 in 2000 anti-mouse (Bcl-2) and 1 in 10,000 anti-mouse (β-tubulin). ECL-plus (GE Healthcare) was used to visualise bands. Following blotting, total protein levels on gels were assessed by Coomassie brilliant blue staining [0.1% (w/v) Coomassie brilliant blue in 50% (v/v) methanol and 7% (v/v) acetic acid] for 2 minutes at room temperature with agitation. Membranes were rinsed briefly in destain [50% (v/v) methanol and 7% (v/v) acetic acid], then washed in destain for 10 minutes before drying and image capture.

Cell blot assay

The cell blot assay is a variation of that developed by Bosque and Prusiner (Bosque and Prusiner, 2000) as described by Lewis et al. (Lewis et al., 2009). PrP was detected using 1 in 10,000 dilution of ICSM18 monoclonal antibody (murine epitope 142-152; D-Gen, UK) in 1% milk PBS-t. Anti-mouse HRP secondary antibody (GE Healthcare) was used at 1 in 10,000 dilution and blots were visualised as above.

MitoSOX assay

Cells were labelled with 5 µM MitoSOX fluorescent indicator probe (Invitrogen) in normal media for 10 minutes under standard incubator conditions. Media was then replaced with fresh, phenol-red-free OptiMEM (Invitrogen) for the duration of the experiment.

MitoTracker staining

Labelling with MitoTracker Green (Invitrogen) was performed with 1 µl MitoTracker in normal media for 30 minutes under standard culture conditions before transfer into phenol-red-free OptiMEM.

Mito-RFP expression

CellLights BacMAM 2.0 Mito-RFP (Invitrogen) at 50 particles per cell was included in normal culture media for no less than 24 hours before cells were to be used.

MTS metabolism assay

5 µl of one-solution MTS reagent (Promega, Sydney, NSW, Australia) was added per 100 µl of culture media in a 96-well plate and absorbency change measured at 492 nm for 2 hours at 37°C. Rates of change were determined from the linear portion of the curve.

Caspase imaging

A 600 µM stock solution of SR-VAD-FMK (Immunochemistry Technologies, Sapphire Biosciences) was prepared in sterile PBS (pH 7.4; Invitrogen) containing 20% (v/v) high-quality sterile-filtered DMSO (Sigma-Aldrich). Cells were plated 24 hours before the start of the assay. 0.6 µM of the SR-VAD-FMK solution was added to Opti-MEM® reduced serum, phenol-red-free media and cells were incubated for 30 minutes under normal growth conditions. The cells were then washed and incubated in fresh Opti-MEM for the duration of the assay.

Annexin-V MACS

Cells were washed in Mg^{2+}/Ca^{2+}-free dPBS and then suspended using trypsin and gently triturated to remove cell clumps. Magnetic

separation was performed as described in the magnetic-activated cell sorting (MACS) protocol (Miltenyi Biotec, Sydney, NSW, Australia). Briefly, cells were centrifuged for 10 minutes at 300 ***g***, resuspended in 80 µl of binding buffer (Miltenyi Biotec) and 20 µl of MACS Annexin V Microbeads (Miltenyi Biotec) added. After 15 minutes incubation at 4°C, the cells were washed in 10 equivalent volumes of binding buffer, centrifuged for 10 minutes at 300 ***g*** and resuspended in 500 µl of binding buffer. MS columns (Miltenyi Biotec) were equilibrated with 500 µl of binding buffer. Labelled cells were applied to the column in a magnetic field and washed twice with 1 ml of binding buffer. The columns were removed from the magnet and cells eluted in 1 ml of binding buffer. These samples were then centrifuged for 5 minutes at 300 ***g*** and resuspended in OptiMEM media. Both annexin-V-labelled and unlabelled fractions were transferred into fresh media for use in ensuing experiments, which were carried out immediately to avoid loss of viability of the annexin-V-positive fraction.

Indirect immunofluorescence

Cells were grown in chambered coverslips (Nunc, Invitrogen) in normal media. Transfections or dye incubations were carried out before fixing. Cells were fixed in 4% (v/v) paraformaldehyde/PBS for 30 minutes and then permeabilised in PBS with 0.1% (v/v) Triton X-100 for 10 minutes. Coverslips were blocked in PBS with 10% FBS (v/v) and 1% (w/v) BSA for 30 minutes. Primary antibodies were diluted in PBS-FBS as appropriate (SOD1, 1 in 500; SOD2, 1 in 250, Abcam; neurofilament-L, 1 in 50, Stem Cell Technologies) and applied overnight at 4°C. Secondary Alexa-Fluor-488/647-conjugated antibodies (Invitrogen) were diluted 1 in 250 in PBS-FBS and were applied for 1 hour at room temperature. Coverslips were coated with Prolong-Gold mounting media (Invitrogen). Fluorophore-stained coverslips were protected from light at all times.

Densitometry and statistical analyses

Luminescent signals of bands on western blots were captured using a Las-3000 intelligent dark box (FujiFilm, Berthold, VIC, Australia) and the intensity quantified, after the subtraction of background, by ImageJ 1.38x. Statistical analyses were carried out using GraphPad Prism 4 or Minitab15 statistical software. Graphs represent the mean and standard error of the mean (s.e.m.) of four independent experiments unless otherwise stated. Primary statistical tests are stated in the text; for one-way ANOVA analysis Tukey's secondary test was applied and Bonferroni's secondary testing was used for two-way ANOVA. Microscope images were captured using a Nikon Eclipse TE2000-E epi-fluorescence microscope (Nikon-Roper Scientific, Coherent Scientific, Adelaide, SA, Australia). All image parameters were maintained throughout an experiment, across all conditions, and the channels of probes sensitive to photo-oxidation were collected before other channels. For imaging data the '*n*' represents independent experiments, which each included capturing sufficient fields to analyse >30 cells per experiment. Cell intensity analysis was done using Nikon NIS-elements 3.0 software with regions of interest used to gate individual cells.

ACKNOWLEDGEMENTS

The authors acknowledge Prof. Andrew Hill for the kind gift of the pIRES vector containing the PrP open reading frames and Dr Simon Drew for the SR-VAD-FMK reagent, and also thank Dr Victoria Lawson and Dr Marcus Brazier for helpful discussions.

COMPETING INTERESTS

The authors declare that they do not have any competing or financial interests.

AUTHOR CONTRIBUTIONS

C.L.H. and S.J.C. conceived the study and developed the experimental design. L.S., V.L. and C.L.H. carried out the experiments. C.L.H. and L.S. wrote the manuscript. S.J.C. and V.L. critically revised the manuscript.

FUNDING

This work was funded by a National Health and Medical Research Council (NH&MRC) program grant (#628946) and a Brain Foundation research grant. S.J.C. is funded by an NH&MRC Practitioner Fellowship (#APP1005816). L.S. is funded in part by a Carol Willesee Foundation Ph.D. scholarship. V.L. is supported by an NH&MRC Training Fellowship (#567123).

SUPPLEMENTARY MATERIAL

Supplementary material for this article is available at http://dmm.biologists.org/lookup/suppl/doi:10.1242/dmm.010678/-/DC1

REFERENCES

Akhtar, S., Grizenkova, J., Wenborn, A., Hummerich, H., Fernandez de Marco, M., Brandner, S., Collinge, J. and Lloyd, S. E. (2013). Sod1 deficiency reduces incubation time in mouse models of prion disease. *PLoS ONE* **8**, e54454.

Bosque, P. J. and Prusiner, S. B. (2000). Cultured cell sublines highly susceptible to prion infection. *J. Virol.* **74**, 4377-4386.

Brazier, M. W., Lewis, V., Ciccotosto, G. D., Klug, G. M., Lawson, V. A., Cappai, R., Ironside, J. W., Masters, C. L., Hill, A. F., White, A. R. et al. (2006). Correlative studies support lipid peroxidation is linked to PrP(res) propagation as an early primary pathogenic event in prion disease. *Brain Res. Bull.* **68**, 346-354.

Brazier, M. W., Doctrow, S. R., Masters, C. L. and Collins, S. J. (2008). A manganese-superoxide dismutase/catalase mimetic extends survival in a mouse model of human prion disease. *Free Radic. Biol. Med.* **45**, 184-192.

Brown, D. R. and Besinger, A. (1998). Prion protein expression and superoxide dismutase activity. *Biochem. J.* **334**, 423-429.

Brown, D. R., Schulz-Schaeffer, W. J., Schmidt, B. and Kretzschmar, H. A. (1997). Prion protein-deficient cells show altered response to oxidative stress due to decreased SOD-1 activity. *Exp. Neurol.* **146**, 104-112.

Brown, D. R., Wong, B. S., Hafiz, F., Clive, C., Haswell, S. J. and Jones, I. M. (1999). Normal prion protein has an activity like that of superoxide dismutase. *Biochem. J.* **344**, 1-5.

Büeler, H., Aguzzi, A., Sailer, A., Greiner, R. A., Autenried, P., Aguet, M. and Weissmann, C. (1993). Mice devoid of PrP are resistant to scrapie. *Cell* **73**, 1339-1347.

Carrì, M. T. and Cozzolino, M. (2011). SOD1 and mitochondria in ALS: a dangerous liaison. *J. Bioenerg. Biomembr.* **43**, 593-599.

Cheng, E. H., Kirsch, D. G., Clem, R. J., Ravi, R., Kastan, M. B., Bedi, A., Ueno, K. and Hardwick, J. M. (1997). Conversion of Bcl-2 to a Bax-like death effector by caspases. *Science* **278**, 1966-1968.

Choi, S. I., Ju, W. K., Choi, E. K., Kim, J., Lea, H. Z., Carp, R. I., Wisniewski, H. M. and Kim, Y. S. (1998). Mitochondrial dysfunction induced by oxidative stress in the brains of hamsters infected with the 263 K scrapie agent. *Acta Neuropathol.* **96**, 279-286.

Drew, S. C., Haigh, C. L., Klemm, H. M., Masters, C. L., Collins, S. J., Barnham, K. J. and Lawson, V. A. (2011). Optical imaging detects apoptosis in the brain and peripheral organs of prion-infected mice. *J. Neuropathol. Exp. Neurol.* **70**, 143-150.

Fischer, M., Rülicke, T., Raeber, A., Sailer, A., Moser, M., Oesch, B., Brandner, S., Aguzzi, A. and Weissmann, C. (1996). Prion protein (PrP) with amino-proximal deletions restoring susceptibility of PrP knockout mice to scrapie. *EMBO J.* **15**, 1255-1264.

Freixes, M., Rodríguez, A., Dalfó, E. and Ferrer, I. (2006). Oxidation, glycoxidation, lipoxidation, nitration, and responses to oxidative stress in the cerebral cortex in Creutzfeldt-Jakob disease. *Neurobiol. Aging* **27**, 1807-1815.

Fukuuchi, T., Doh-Ura, K., Yoshihara, S. and Ohta, S. (2006). Metal complexes with superoxide dismutase-like activity as candidates for anti-prion drug. *Bioorg. Med. Chem. Lett.* **16**, 5982-5987.

Goldsteins, G., Keksa-Goldsteine, V., Ahtoniemi, T., Jaronen, M., Arens, E., Akerman, K., Chan, P. H. and Koistinaho, J. (2008). Deleterious role of superoxide dismutase in the mitochondrial intermembrane space. *J. Biol. Chem.* **283**, 8446-8452.

Haigh, C. L., Lewis, V. A., Vella, L. J., Masters, C. L., Hill, A. F., Lawson, V. A. and Collins, S. J. (2009). PrPC-related signal transduction is influenced by copper, membrane integrity and the alpha cleavage site. *Cell Res.* **19**, 1062-1078.

Haigh, C. L., McGlade, A. R., Lewis, V., Masters, C. L., Lawson, V. A. and Collins, S. J. (2011). Acute exposure to prion infection induces transient oxidative stress progressing to be cumulatively deleterious with chronic propagation in vitro. *Free Radic. Biol. Med.* **51**, 594-608.

Hinerfeld, D., Traini, M. D., Weinberger, R. P., Cochran, B., Doctrow, S. R., Harry, J. and Melov, S. (2004). Endogenous mitochondrial oxidative stress: neurodegeneration,

proteomic analysis, specific respiratory chain defects, and efficacious antioxidant therapy in superoxide dismutase 2 null mice. *J. Neurochem.* **88**, 657-667.

Holley, A. K., Bakthavatchalu, V., Velez-Roman, J. M. and St Clair, D. K. (2011). Manganese superoxide dismutase: guardian of the powerhouse. *Int. J. Mol. Sci.* **12**, 7114-7162.

Jesionek-Kupnicka, D., Buczyński, J., Kordek, R., Sobów, T., Kłoszewska, I., Papierz, W. and Liberski, P. P. (1997). Programmed cell death (apoptosis) in Alzheimer's disease and Creutzfeldt-Jakob disease. *Folia Neuropathol.* **35**, 233-235.

Kawamata, H. and Manfredi, G. (2010). Import, maturation, and function of SOD1 and its copper chaperone CCS in the mitochondrial intermembrane space. *Antioxid. Redox Signal.* **13**, 1375-1384.

Klamt, F., Dal-Pizzol, F., Conte da Frota, M. L., Jr, Walz, R., Andrades, M. E., da Silva, E. G., Brentani, R. R., Izquierdo, I. and Fonseca Moreira, J. C. (2001). Imbalance of antioxidant defense in mice lacking cellular prion protein. *Free Radic. Biol. Med.* **30**, 1137-1144.

Kristiansen, M., Messenger, M. J., Klöhn, P. C., Brandner, S., Wadsworth, J. D. F., Collinge, J. and Tabrizi, S. J. (2005). Disease-related prion protein forms aggresomes in neuronal cells leading to caspase activation and apoptosis. *J. Biol. Chem.* **280**, 38851-38861.

Kurschner, C. and Morgan, J. I. (1995). The cellular prion protein (PrP) selectively binds to Bcl-2 in the yeast two-hybrid system. *Brain Res. Mol. Brain Res.* **30**, 165-168.

Lawson, V. A., Vella, L. J., Stewart, J. D., Sharples, R. A., Klemm, H., Machalek, D. M., Masters, C. L., Cappai, R., Collins, S. J. and Hill, A. F. (2008). Mouse-adapted sporadic human Creutzfeldt-Jakob disease prions propagate in cell culture. *Int. J. Biochem. Cell Biol.* **40**, 2793-2801.

Lawson, V. A., Haigh, C. L., Roberts, B., Kenche, V. B., Klemm, H. M., Masters, C. L., Collins, S. J., Barnham, K. J. and Drew, S. C. (2010). Near-infrared fluorescence imaging of apoptotic neuronal cell death in a live animal model of prion disease. *ACS Chem. Neurosci.* **1**, 720-727.

Lebovitz, R. M., Zhang, H., Vogel, H., Cartwright, J., Jr, Dionne, L., Lu, N., Huang, S. and Matzuk, M. M. (1996). Neurodegeneration, myocardial injury, and perinatal death in mitochondrial superoxide dismutase-deficient mice. *Proc. Natl. Acad. Sci. USA* **93**, 9782-9787.

Lee, D. W., Sohn, H. O., Lim, H. B., Lee, Y. G., Kim, Y. S., Carp, R. I. and Wisniewski, H. M. (1999). Alteration of free radical metabolism in the brain of mice infected with scrapie agent. *Free Radic. Res.* **30**, 499-507.

Lewis, V., Hill, A. F., Haigh, C. L., Klug, G. M., Masters, C. L., Lawson, V. A. and Collins, S. J. (2009). Increased proportions of C1 truncated prion protein protect against cellular M1000 prion infection. *J. Neuropathol. Exp. Neurol.* **68**, 1125-1135.

Li, X. L., Wang, G. R., Jing, Y. Y., Pan, M. M., Dong, C. F., Zhou, R. M., Wang, Z. Y., Shi, Q., Gao, C. and Dong, X. P. (2011). Cytosolic PrP induces apoptosis of cell by disrupting microtubule assembly. *J. Mol. Neurosci.* **43**, 316-325.

Lyamzaev, K. G., Nepryakhina, O. K., Saprunova, V. B., Bakeeva, L. E., Pletjushkina, O. Y., Chernyak, B. V. and Skulachev, V. P. (2008). Novel mechanism of elimination of malfunctioning mitochondria (mitoptosis): formation of mitoptotic bodies and extrusion of mitochondrial material from the cell. *Biochim. Biophys. Acta* **1777**, 817-825.

Mattei, V., Matarrese, P., Garofalo, T., Tinari, A., Gambardella, L., Ciarlo, L., Manganelli, V., Tasciotti, V., Misasi, R., Malorni, W. et al. (2011). Recruitment of cellular prion protein to mitochondrial raft-like microdomains contributes to apoptosis execution. *Mol. Biol. Cell* **22**, 4842-4853.

Melov, S., Schneider, J. A., Day, B. J., Hinerfeld, D., Coskun, P., Mirra, S. S., Crapo, J. D. and Wallace, D. C. (1998). A novel neurological phenotype in mice lacking mitochondrial manganese superoxide dismutase. *Nat. Genet.* **18**, 159-163.

Mijaljica, D., Prescott, M. and Devenish, R. J. (2010). Mitophagy and mitoptosis in disease processes. *Methods Mol. Biol.* **648**, 93-106.

Mouillet-Richard, S., Schneider, B., Pradines, E., Pietri, M., Ermonval, M., Grassi, J., Richards, J. G., Mutel, V., Launay, J. M. and Kellermann, O. (2007). Cellular prion protein signaling in serotonergic neuronal cells. *Ann. New York Acad. Sci.* **1096**, 106-119.

Nakajima, A., Kurihara, H., Yagita, H., Okumura, K. and Nakano, H. (2008). Mitochondrial extrusion through the cytoplasmic vacuoles during cell death. *J. Biol. Chem.* **283**, 24128-24135.

Pardo, M., Melendez, J. A. and Tirosh, O. (2006). Manganese superoxide dismutase inactivation during Fas (CD95)-mediated apoptosis in Jurkat T cells. *Free Radic. Biol. Med.* **41**, 1795-1806.

Park, J. H., Kim, B. H., Park, S. J., Jin, J. K., Jeon, Y. C., Wen, G. Y., Shin, H. Y., Carp, R. I. and Kim, Y. S. (2011). Association of endothelial nitric oxide synthase and mitochondrial dysfunction in the hippocampus of scrapie-infected mice. *Hippocampus* **21**, 319-333.

Paterson, A. W., Curtis, J. C. and Macleod, N. K. (2008). Complex I specific increase in superoxide formation and respiration rate by PrP-null mouse brain mitochondria. *J. Neurochem.* **105**, 177-191.

Prusiner, S. B. (1982). Novel proteinaceous infectious particles cause scrapie. *Science* **216**, 136-144.

Puig, B. and Ferrer, I. (2001). Cell death signaling in the cerebellum in Creutzfeldt-Jakob disease. *Acta Neuropathol.* **102**, 207-215.

Rachidi, W., Vilette, D., Guiraud, P., Arlotto, M., Riondel, J., Laude, H., Lehmann, S. and Favier, A. (2003). Expression of prion protein increases cellular copper binding and antioxidant enzyme activities but not copper delivery. *J. Biol. Chem.* **278**, 9064-9072.

Rambold, A. S., Miesbauer, M., Rapaport, D., Bartke, T., Baier, M., Winklhofer, K. F. and Tatzelt, J. (2006). Association of Bcl-2 with misfolded prion protein is linked to the toxic potential of cytosolic PrP. *Mol. Biol. Cell* **17**, 3356-3368.

Sakudo, A., Lee, D. C., Nishimura, T., Li, S., Tsuji, S., Nakamura, T., Matsumoto, Y., Saeki, K., Itohara, S., Ikuta, K. et al. (2005). Octapeptide repeat region and N-terminal half of hydrophobic region of prion protein (PrP) mediate PrP-dependent activation of superoxide dismutase. *Biochem. Biophys. Res. Commun.* **326**, 600-606.

Sam, F., Kerstetter, D. L., Pimental, D. R., Mulukutla, S., Tabaee, A., Bristow, M. R., Colucci, W. S. and Sawyer, D. B. (2005). Increased reactive oxygen species production and functional alterations in antioxidant enzymes in human failing myocardium. *J. Card. Fail.* **11**, 473-480.

Schneider, B., Mutel, V., Pietri, M., Ermonval, M., Mouillet-Richard, S. and Kellermann, O. (2003). NADPH oxidase and extracellular regulated kinases 1/2 are targets of prion protein signaling in neuronal and nonneuronal cells. *Proc. Natl. Acad. Sci. USA* **100**, 13326-13331.

Scott, J. L., Gabrielides, C., Davidson, R. K., Swingler, T. E., Clark, I. M., Wallis, G. A., Boot-Handford, R. P., Kirkwood, T. B. L., Taylor, R. W. and Young, D. A. (2010). Superoxide dismutase downregulation in osteoarthritis progression and end-stage disease. *Ann. Rheum. Dis.* **69**, 1502-1510.

Singh, N., Singh, A., Das, D. and Mohan, M. L. (2010). Redox control of prion and disease pathogenesis. *Antioxid. Redox Signal.* **12**, 1271-1294.

Sisková, Z., Mahad, D. J., Pudney, C., Campbell, G., Cadogan, M., Asuni, A., O'Connor, V. and Perry, V. H. (2010). Morphological and functional abnormalities in mitochondria associated with synaptic degeneration in prion disease. *Am. J. Pathol.* **177**, 1411-1421.

Steele, A. D., King, O. D., Jackson, W. S., Hetz, C. A., Borkowski, A. W., Thielen, P., Wollmann, R. and Lindquist, S. (2007). Diminishing apoptosis by deletion of Bax or overexpression of Bcl-2 does not protect against infectious prion toxicity in vivo. *J. Neurosci.* **27**, 13022-13027.

Steinacker, P., Hawlik, A., Lehnert, S., Jahn, O., Meier, S., Görz, E., Braunstein, K. E., Krzovska, M., Schwalenstöcker, B., Jesse, S. et al. (2010). Neuroprotective function of cellular prion protein in a mouse model of amyotrophic lateral sclerosis. *Am. J. Pathol.* **176**, 1409-1420.

Tinari, A., Garofalo, T., Sorice, M., Esposti, M. D. and Malorni, W. (2007). Mitoptosis: different pathways for mitochondrial execution. *Autophagy* **3**, 282-284.

Weissmann, C., Büeler, H., Fischer, M., Sailer, A., Aguzzi, A. and Aguet, M. (1994). PrP-deficient mice are resistant to scrapie. *Ann. New York Acad. Sci.* **724**, 235-240.

Wong, B. S., Brown, D. R., Pan, T., Whiteman, M., Liu, T., Bu, X., Li, R., Gambetti, P., Olesik, J., Rubenstein, R. et al. (2001). Oxidative impairment in scrapie-infected mice is associated with brain metals perturbations and altered antioxidant activities. *J. Neurochem.* **79**, 689-698.